

Cell Stem Cell, Volume 12

Supplemental Information

Regulation of Glycolysis by Pdk Functions

as a Metabolic Checkpoint for Cell Cycle

Quiescence in Hematopoietic Stem Cells

Keiyo Takubo, Go Nagamatsu, Chiharu I. Kobayashi, Ayako Nakamura-Ishizu, Hiroshi Kobayashi, Eiji Ikeda, Nobuhito Goda, Yasmeen Rahimi, Randall S. Johnson, Tomoyoshi Soga, Atsushi Hirao, Makoto Suematsu, and Toshio Suda

Inventory of Supplemental Information

Figure S1, related to Figure 1

Figure S2, related to Figure 2

Figure S3, related to Figure 3

Figure S4, related to Figure 4

Figure S5, related to Figure 5

Figure S6, related to Figure 6

Figure S7, related to Figure 7

Figure S1

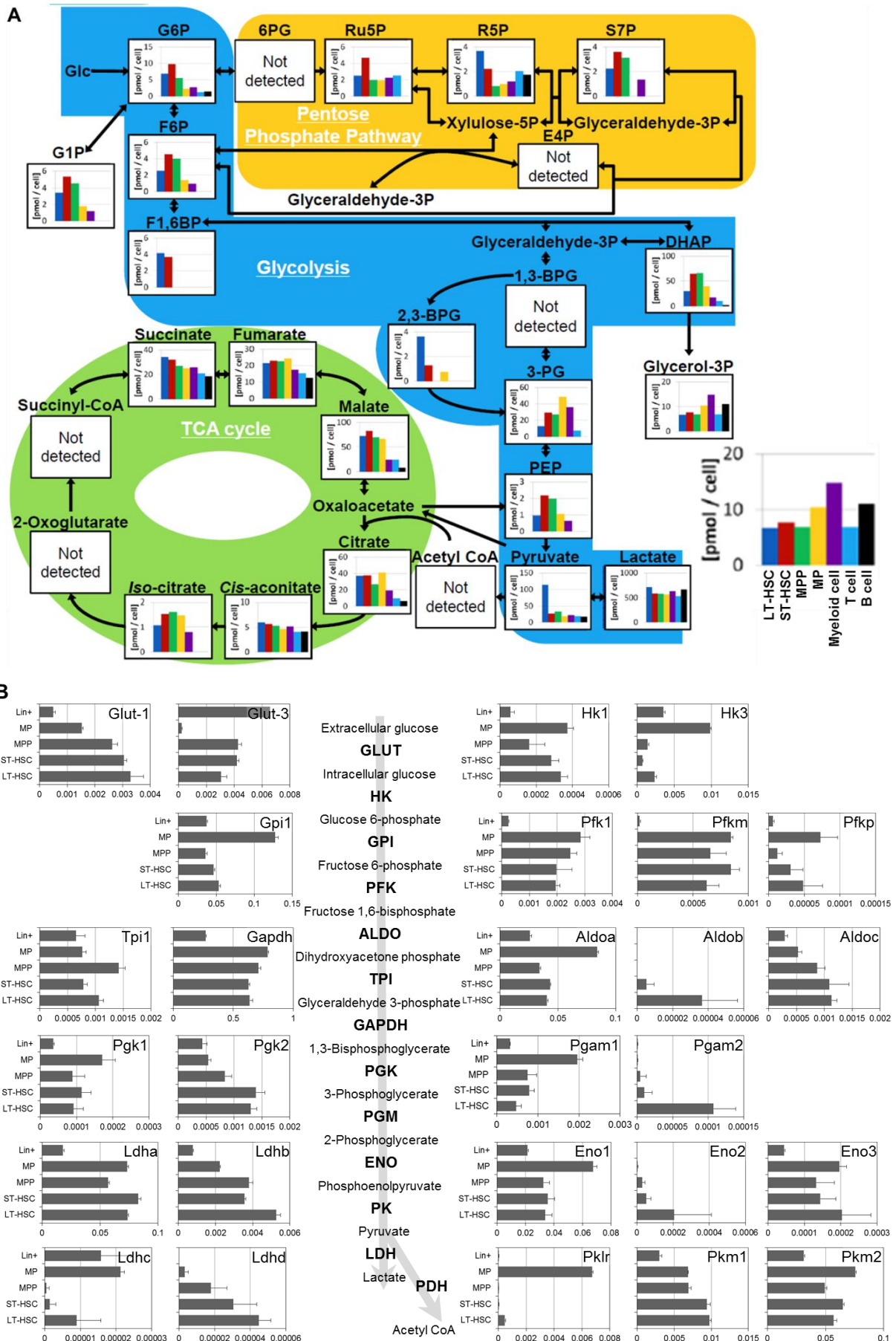


Figure S1, related to Figure 1

Metabolomic profiling of central carbon metabolism in HSCs and their progeny.

A, Quantification of metabolites in central carbon metabolism based on CE-TOFMS analysis. Bar graphs for independent metabolites plotted in the central carbon metabolism map are (from left to right): long-term (LT)-hematopoietic stem cells (HSCs) (CD34⁻Flt3⁻ LSK cells; blue bars), short-term (ST)-HSCs (CD34⁺Flt3⁻ LSK cells; red bars), multipotent progenitors (MPPs) (CD34⁺Flt3⁺ LSK cells; green bars), myeloid progenitors (MPs; Lin⁻ c-Kit⁺ Sca-1⁻ cells; yellow bars), Gr-1/Mac-1⁺ myeloid cells (purple bars), CD4/CD8⁺ T cells (sky blue bars), and B220⁺ B lymphocytes (black bars). Metabolites not detected in any fraction are indicated as “Not detected” in the metabolic map. Data is representative of two independent experiments.

B, Expression levels of glycolytic enzymes in various hematopoietic compartments. Relative mRNA expression of glycolytic enzymes in wild-type BM fractions (LT-HSC, ST-HSC, MPP, MP, or Lin⁺). Expression levels are normalized to β -actin expression (mean \pm SD, n=4).

Figure S2

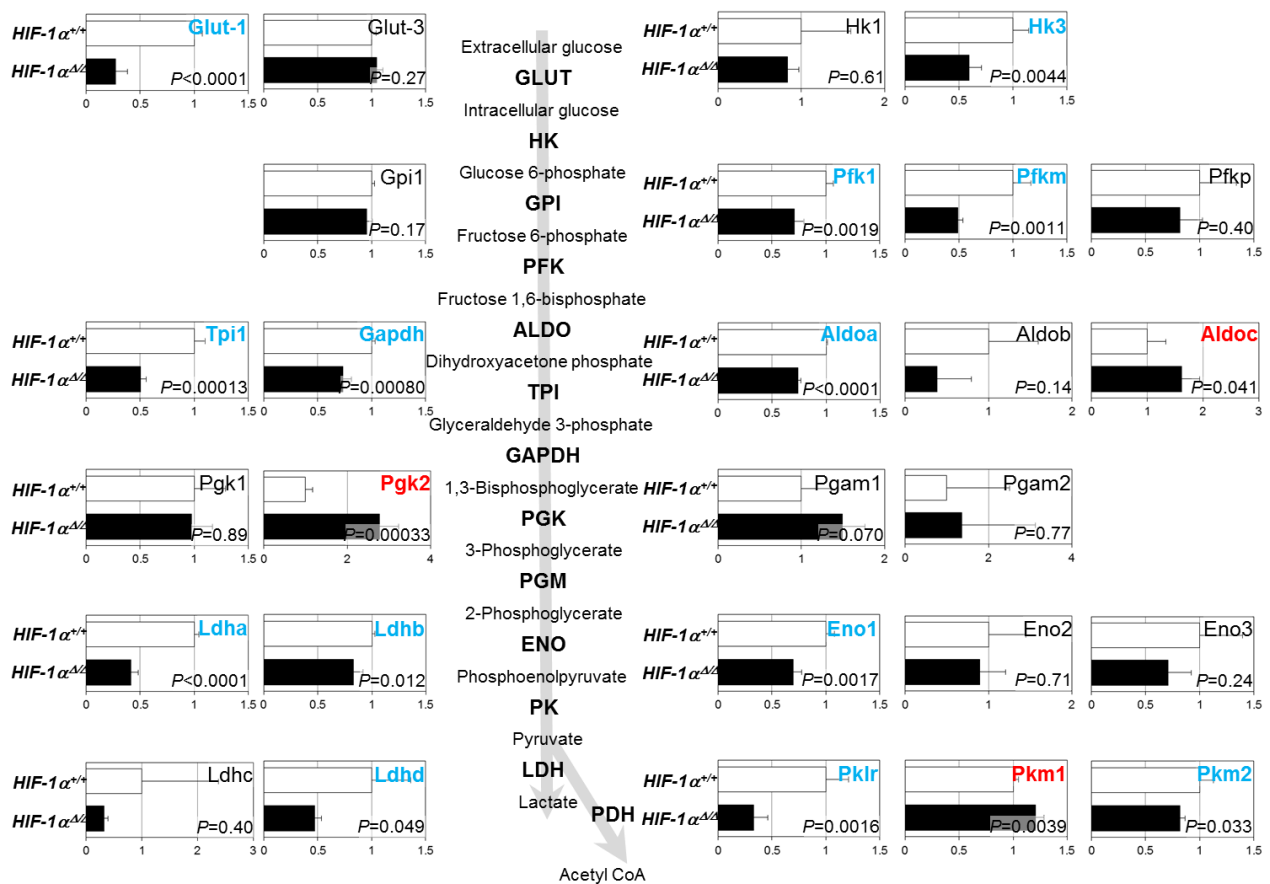


Figure S2, related to Figure 2

Expression levels of glycolytic enzymes in *HIF-1α^{ΔΔ}* LT-HSCs

Relative mRNA expression of glycolytic enzymes in CD34⁻ Flt-3⁻ LSK samples from *HIF-1α^{+/+}* (open bars) or *HIF-1α^{ΔΔ}* (closed bars) mice. Each value is normalized to β-actin expression and expressed as fold-induction compared to levels (set to 1) detected in *HIF-1α^{+/+}* CD34⁻ Flt-3⁻ LSK samples (open bars) (mean ± SD, n=4). Genes significantly downregulated or upregulated ($P < 0.05$) in *HIF-1α^{ΔΔ}* compared to *HIF-1α^{+/+}* samples are shown in blue or red, respectively.

Figure S3

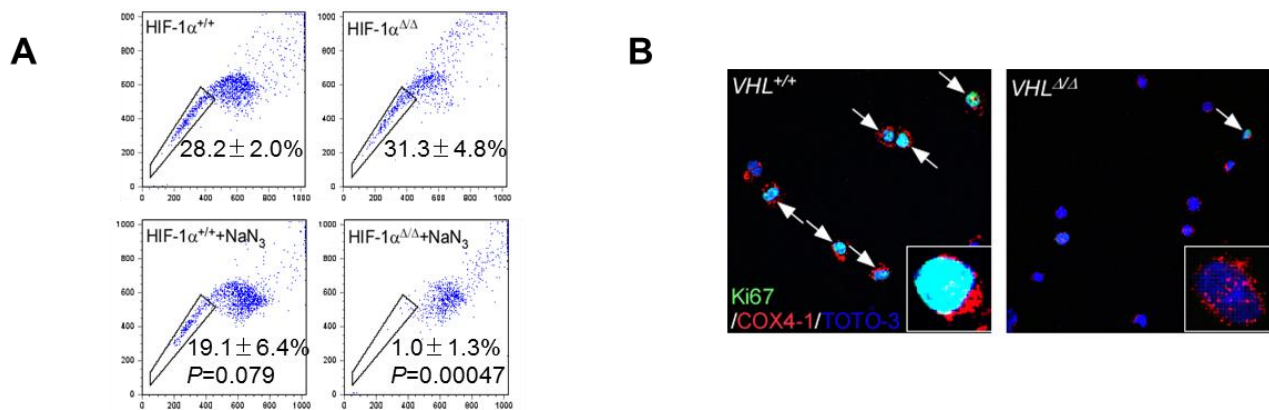


Figure S3, related to Figure 3

Metabolic alterations in HIF- α ^{Δ/Δ} or VHL ^{Δ/Δ} primitive hematopoietic cells

A, Flow cytometric analysis of the effects of 20mM NaN₃ treatment on ATP-transporter-mediated dye exclusion from HIF-1 α ^{+/+} or HIF-1 α ^{Δ/Δ} LSK cells. The enclosed region in the FACS plots represents the mean percentage of the LSK-gated Side Population (mean \pm SD, n=3).

B, Immunocytochemical staining of Ki67 (green), COX4-1 (red), and TOTO-3 (blue) in VHL^{+/+} or VHL ^{Δ/Δ} LSK cells. Arrows indicate cells positive for both green and red signals in the nucleus. Insets show representative cells from each LSK sample.

Figure S4

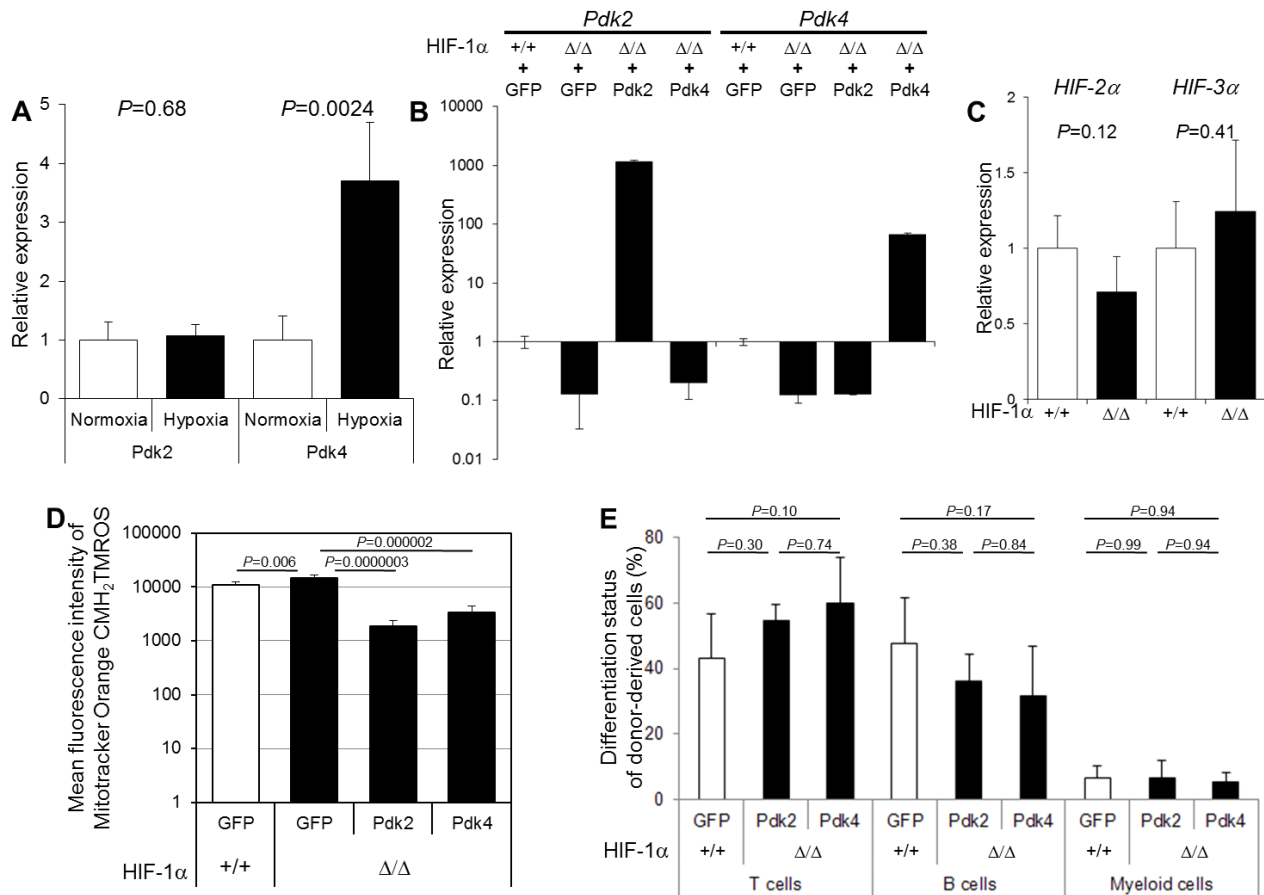


Figure S4, related to Figure 4

Suppression of ROS production and efficient multilineage differentiation by Pdk2 in HIF-1α^{Δ/Δ} HSCs

A, Relative levels of Pdk2 or Pdk4 mRNAs in LT-HSCs (CD34⁻ Flt-3⁻ LSK cells) exposed to normoxia (20%O₂) or hypoxia (1%O₂) for 14 hours (n=4). Each value is normalized to β-actin expression and expressed as fold-induction compared to levels (set to 1) detected in normoxia-treated LT-HSC samples (mean ± SD, n=4).

B, Relative levels of Pdk2 or Pdk4 mRNAs in LT-HSCs (CD34⁻ Flt-3⁻ LSK cells) from HIF-1α^{+/+} or HIF-1α^{Δ/Δ} mice transduced with GFP, Pdk2 or Pdk4 retroviruses (n=4). Each value is normalized to β-actin expression and expressed as fold-induction compared to levels (set to 1) detected in GFP-transduced HIF-1α^{+/+} LT-HSC samples (mean ± SD, n=4).

C, Relative levels of HIF-2α or HIF-3α mRNAs in LT-HSCs (CD34⁻ Flt-3⁻ LSK cells) from HIF-1α^{+/+} or HIF-1α^{Δ/Δ} mice (n=4). Each value is normalized to β-actin expression and expressed as fold-induction compared to levels (set to 1) detected in HIF-1α^{+/+} LT-HSC samples (mean ± SD, n=4).

D, Mitochondrial ROS detection by Mitotracker Orange CMH₂TMROS in LSK cells transduced with GFP, Pdk2 or Pdk4 retroviruses (n=5). Data are presented as the mean fluorescence intensity \pm SEM.

E, Differentiation status (CD4/CD8⁺ T cells, B220⁺ B cells, or Mac-1/Gr-1⁺ myeloid cells) of donor-derived (Ly5.2⁺) PB cells in primary BMT recipients of GFP virus-transduced HIF-1 $\alpha^{+/+}$ LSK cells, GFP virus-transduced HIF-1 $\alpha^{\Delta/\Delta}$ LSK cells, Pdk2 virus-transduced HIF-1 $\alpha^{\Delta/\Delta}$ LSK cells, or Pdk4 virus-transduced HIF-1 $\alpha^{\Delta/\Delta}$ LSK cells (mean \pm SD, n=5).

Figure S5

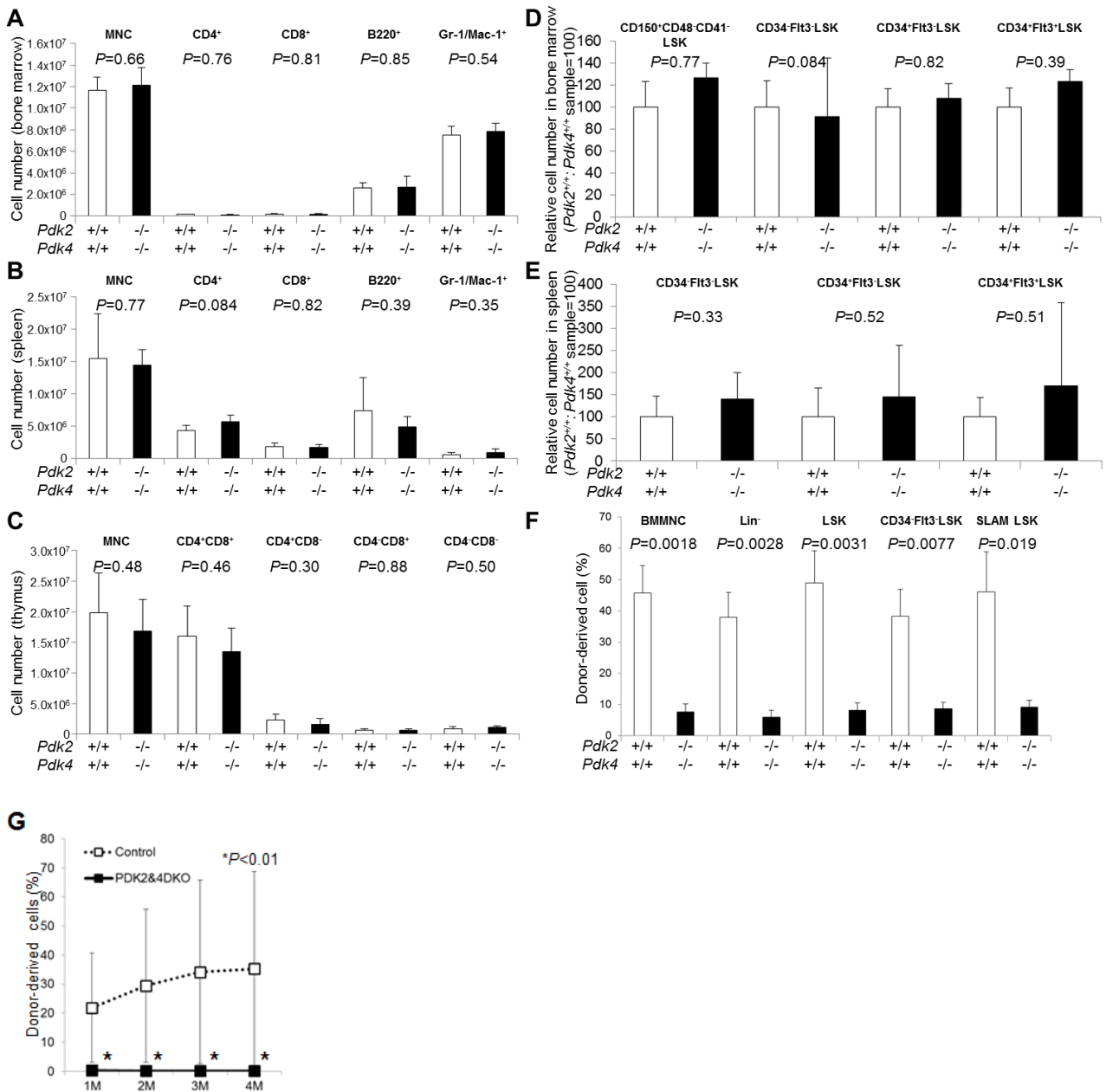


Figure S5, related to Figure 5

Number of differentiated and primitive hematopoietic cells in *Pdk2*^{-/-}; *Pdk4*^{-/-} mice

A-C, Number of MNCs or cells from various differentiated cell fractions in BM (**A**), spleen (**B**) or thymus (**C**) of *Pdk2*^{-/-}; *Pdk4*^{-/-} mice (mean ± SD, n=4).

D, E, Number of cells in primitive cell fractions including CD34⁺Fit3⁻ LSK, CD34⁺Fit3⁻ LSK, or CD34⁺Fit3⁺ LSK in BM (**D**) or spleen (**E**) of *Pdk2*^{-/-}; *Pdk4*^{-/-} mice (mean ± SD, n=4).

F, Donor-derived (Ly5.2+) BM MNC, Lin⁻, LSK, CD34-Flt3⁻ LSK or SLAM-LSK chimerism in secondary BMT recipients of control (open bars) or *Pdk2*^{-/-}:*Pdk4*^{-/-} (closed bars) LT-HSCs 4 months after primary BMT (mean ± SEM, n = 10).

G, PB chimerism in tertiary recipients of BM derived from secondary recipients of control (open boxes) or *Pdk2*^{-/-}:*Pdk4*^{-/-} (closed boxes) MNCs, at indicated times after BMT (mean ± SD, n = 10).

Figure S6

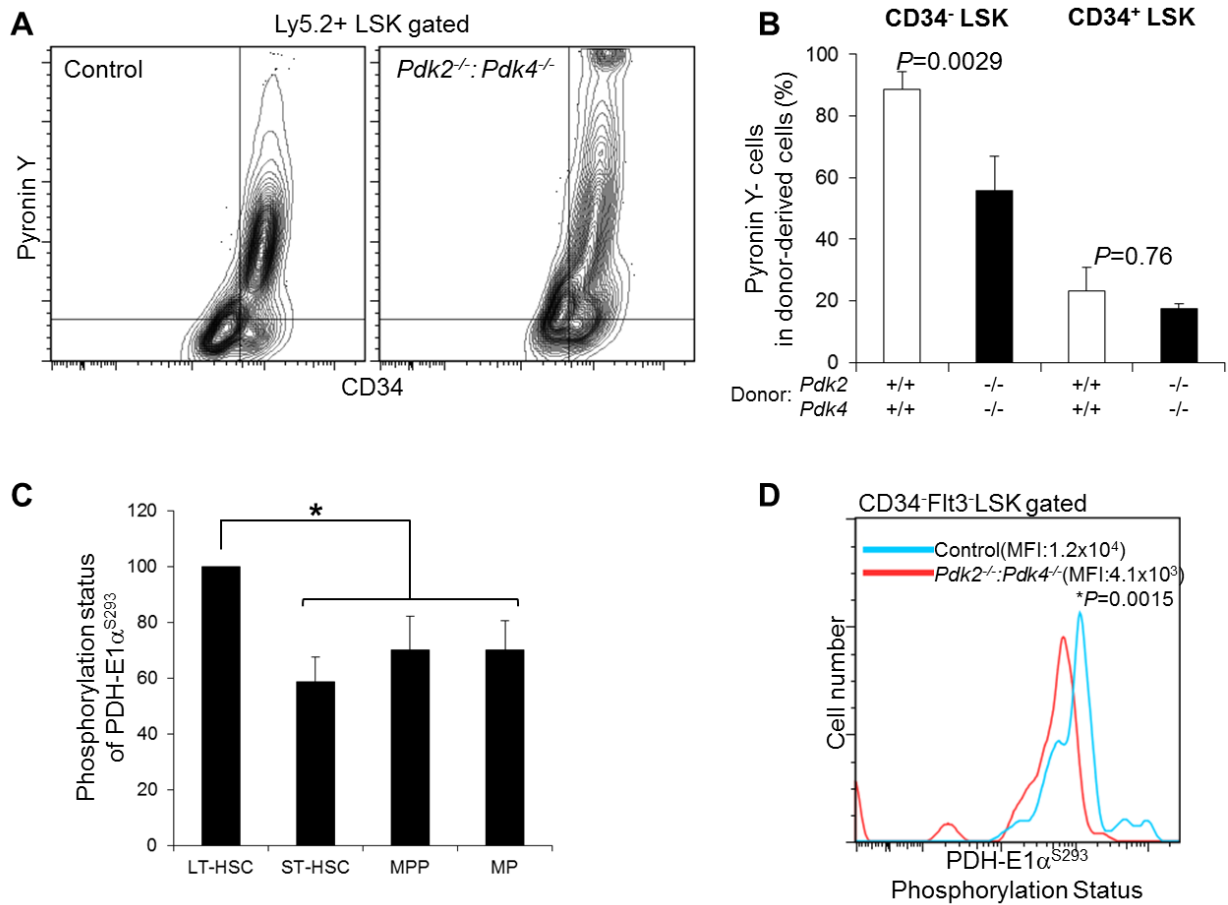


Figure S6, related to Figure 6

***Pdk2^{-/-}; Pdk4^{-/-}* LT-HSCs lose quiescence in a normal microenvironment**

A, Representative flow cytometric plot of Pyronin Y analysis in the LSK gated fraction of control or *Pdk2^{-/-}; Pdk4^{-/-}* BM mice.

B, Summary of flow cytometric Pyronin Y analysis of CD34⁻ LSK or CD34⁺ LSK fractions in control or *Pdk2^{-/-}; Pdk4^{-/-}* BM mice (mean \pm SD, n=3).

C, Detection of phosphorylated PDH-E1 α^{S293} by intracellular flow cytometry in LT-HSC, ST-HSC, MPP, and MP fractions. Mean fluorescence intensity (MFI) of anti-phosphorylated PDH-E1 α^{S293} antibody staining is normalized to MFI detected in the LT-HSC fraction (mean \pm SD, n=3, **P*<0.001).

D, Representative histogram comparing phosphorylated PDH-E1 α^{S293} levels using intracellular flow cytometry analysis of control versus *Pdk2^{-/-}; Pdk4^{-/-}* LT-HSCs. Average MFIs are shown (n=3, **P*=0.0015).

Figure S7

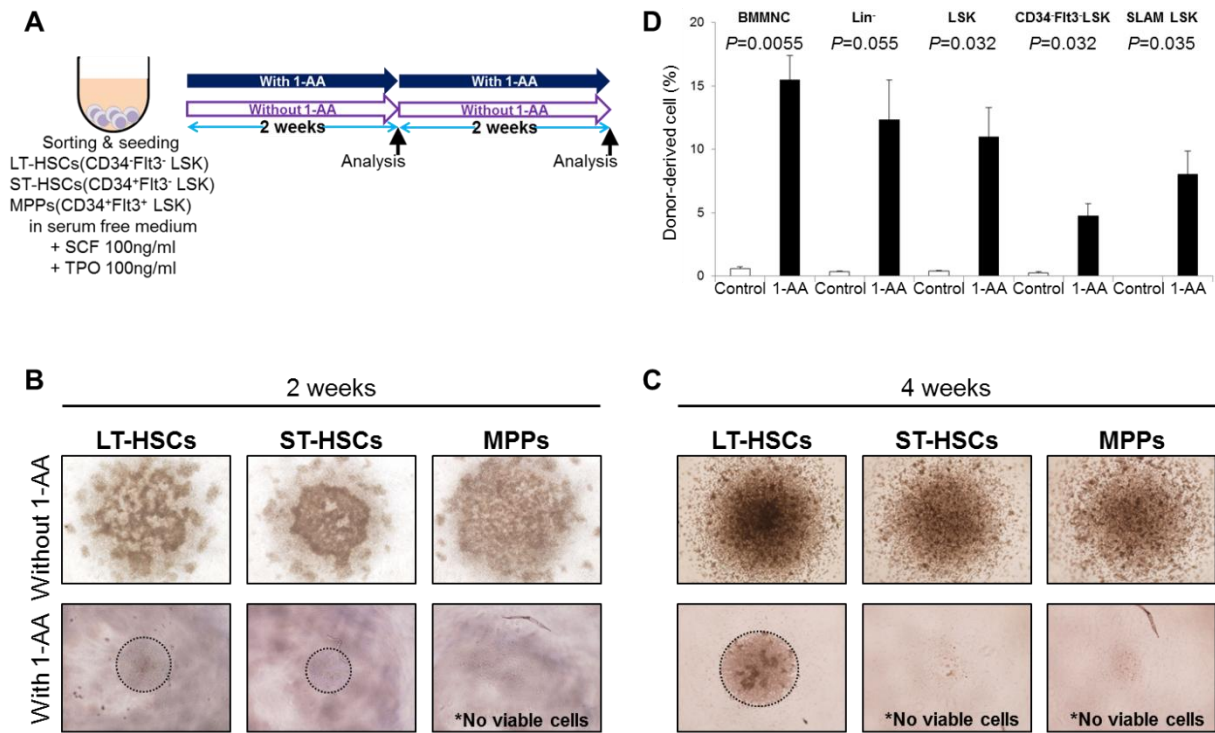


Figure S7, related to Figure 7

Effect of 1-AA on colony formation of LT-HSCs, ST-HSCs or MPPs

A, Design of LT-HSC, ST-HSC, or MPP cultures treated without or with 1-AA for 2 or 4 weeks.

B, Light microscopic analysis of colonies cultured 2 weeks from LT-HSC, ST-HSC, or MPP cultures treated with or without 1-AA.

C, Light microscopic analysis of colonies cultured 4 weeks from LT-HSC, ST-HSC, or MPP cultures treated with or without 1-AA.

D, Donor-derived (Ly5.1+) BM MNC, Lin-, LSK, CD34-Fit3- LSK or SLAM-LSK chimerism in primary BMT recipients of control LT-HSCs (open bars) or LT-HSCs treated with 1-AA for 4 weeks (closed bars) 4 months after BMT (mean \pm SEM, n = 4-5).